ORIGINAL RESEARCH

Calcineurin/Nuclear Factor of Activated T Cells–Coupled Vanilliod Transient Receptor Potential Channel 4 Ca^{2+} Sparklets Stimulate Airway Smooth Muscle Cell Proliferation

Limin Zhao[1,2], Michelle N. Sullivan[1], Marlee Chase[1], Albert L. Gonzales[3], and Scott Earley[4]

[1]Vascular Physiology Research Group, Department of Biomedical Sciences, Colorado State University, Fort Collins, Colorado; [2]Henan Provincial People's Hospital of Zhengzhou University, Zhengzhou, Henan, China; [3]Department of Pharmacology, University of Vermont School of Medicine, Burlington, Vermont; and [4]Department of Pharmacology, University of Nevada School of Medicine, Reno, Nevada

Abstract

Proliferation of airway smooth muscle cells (ASMCs) contributes to the remodeling and irreversible obstruction of airways during severe asthma, but the mechanisms underlying this disease process are poorly understood. Here we tested the hypothesis that Ca^{2+} influx through the vanilliod transient receptor potential channel (TRPV) 4 stimulates ASMC proliferation. We found that synthetic and endogenous TRPV4 agonists increase proliferation of primary ASMCs. Furthermore, we demonstrate that Ca^{2+} influx through individual TRPV4 channels produces Ca^{2+} microdomains in ASMCs, called "TRPV4 Ca^{2+} sparklets." We also show that TRPV4 channels colocalize with the Ca^{2+}/calmodulin–dependent protein phosphatase calcineurin in ASMCs. Activated calcineurin dephosphorylates nuclear factor of activated T cells (NFAT) transcription factors cytosolic (c) to allow nuclear translocation and activation of synthetic transcriptional pathways. We show that ASMC proliferation in response to TRPV4 activity is associated with calcineurin-dependent nuclear translocation of the NFATc3 isoform tagged with green florescent protein. Our findings suggest that Ca^{2+} microdomains created by TRPV4 Ca^{2+} sparklets activate calcineurin to stimulate nuclear translocation of NFAT and ASMC proliferation. These findings further suggest that inhibition of TRPV4 could diminish asthma-induced airway remodeling.

Keywords: airway smooth muscle; asthma-induced airway remodeling; nuclear factor of activated T cells; transient receptor potential channel; vanilliod transient receptor potential channel 4 Ca^{2+} sparklet

Clinical Relevance

The research described here demonstrates that activation of the vanilliod transient receptor potential channel 4 causes proliferation of airway smooth muscle cells. This identifies the channel as a possible therapeutic target for the treatment of asthma-induced airway remodeling.

Bronchial asthma, a common, chronic disease, is characterized by airway hyperresponsiveness, inflammation, and obstruction. Rapid, global increases in the incidence of asthma strain healthcare delivery systems, stimulating interest in new therapies to prevent and treat the disease. Thickening of the airway wall, or airway remodeling, is associated with chronic, severe forms of asthma (1). This pathology is responsible for irreversible airway obstruction and steroid-resistant forms of the disease (2). Airway remodeling is a complex disease process resulting from chronic injury and repair mechanisms, characterized by changes in the cellular and molecular composition of the airway wall that include deposition of extracellular matrix, basement membrane thickening, and airway smooth muscle cell (ASMC) hyperplasia and hypertrophy (3). Although proliferation of ASMCs has long been known to be a major contributor to asthma-induced airway remodeling (4), the

(Received in original form September 26, 2013; accepted in final form December 16, 2013)

This work was supported by a Monfort Excellence Award from the Monfort Family Foundation (S.E.) and National Heart, Lung, and Blood Institute grants R01HL091905 (S.E.) and F31HL094145 (A.L.G.).

Correspondence and requests for reprints should be addressed to Scott Earley, Ph.D., Department of Pharmacology/MS 318, University of Nevada School of Medicine, 8 Manville, Reno, NV 89557-0318. E-mail: searley@medicine.nevada.edu

This article has an online supplement, which is accessible from this issue's table of contents at www.atsjournals.org

Am J Respir Cell Mol Biol Vol 50, Iss 6, pp 1064–1075, Jun 2014

Originally Published in Press as DOI: 10.1165/rcmb.2013-0416OC on January 6, 2014
Internet address: www.atsjournals.org

mechanisms underlying this response remain poorly understood.

Proliferation of smooth muscle cells requires a shift from the normally quiescent, contractile state maintained under healthy conditions to a synthetic, noncontractile phenotype during disease (5). The molecular mechanisms underlying this transformation are not fully understood, but it is clear that nuclear factor of activated T cells (NFAT) transcription factors can stimulate hypertrophy and proliferation of smooth muscle cells under pathological conditions (6, 7). The NFAT transcription factor family consists of five members: NFATc1, NFATc2, NFATc3, NFATc4, and NFAT5 (8). NFATc1–4 are homologous, share similar regulatory pathways, and are highly phosphorylated in the cytosol of quiescent cells. In response to specific Ca^{2+} signals, the Ca^{2+}/calmodulin–dependent phosphatase, calcineurin, docks with and dephosphorylates NFATc isoforms to allow nuclear translocation and activation of transcriptional programs leading to cellular proliferation (8). It is not known if NFAT is present in ASMCs or contributes to ASMC proliferation during asthma.

Activation of the calcineurin/NFATc synthetic pathway is Ca^{2+} dependent, but specific types of Ca^{2+} signals activate NFAT in different types of cells. For example, in arterial smooth muscle cells, subcellular regions where Ca^{2+} levels are significantly higher than average cytosolic levels (Ca^{2+} microdomains), rather than global increases in intracellular Ca^{2+}, can stimulate NFATc3-dependent cellular hypertrophy (9). Ca^{2+} influx through persistently active voltage-dependent (Cav1.2) Ca^{2+} channels (10), called "L-type Ca^{2+} channel sparklets" (11), generates the Ca^{2+} microdomains activating NFATc3 in these cells. Ca^{2+} microdomains produced by Ca^{2+} influx through vanilliod transient receptor potential channel (TRPV) 4 channels, called "TRPV4 Ca^{2+} sparklets," have been recorded from vascular endothelial cells (12, 13). TRPV4 Ca^{2+} sparklets are larger in amplitude than L-type Ca^{2+} channel sparklets, but it is not currently known if these signals are present in smooth muscle cells or if such events could contribute to ASMC proliferation and airway remodeling.

We hypothesized that TRPV4 Ca^{2+} sparklets contribute to ASMC proliferation by activating NFAT. Here, we provide evidence that TRPV4 channels are present and active in ASMCs, generate TRPV4 Ca^{2+} sparklets, and are functionally coupled to calcineurin. Furthermore, we show that TRPV4 activity induces nuclear translocation of NFATc3. Our results indicate that Ca^{2+} microdomains created by TRPV4 channels stimulate ASMC proliferation by activating the calcineurin/NFAT pathway, suggesting that TRPV4 may be a new potential target for the treatment of asthma-induced airway remodeling.

Materials and Methods

Primary ASMC Culture

Male Sprague-Dawley rats (250–350 g; Harlan, Indianapolis, IN) were deeply anesthetized with pentobarbital sodium (50 mg intraperitoneal) and killed by exsanguination according to a protocol approved by the Institutional Animal Care and Use Committee of Colorado State University. Primary ASMC cultures were established as follows. Large bronchi dissected from the surrounding parenchyma were washed in cooled physiological saline solution (PSS) (118 mM NaCl, 4.7 mM KCl, 1.2 mM NaH_2PO_4, 25.5 mM $NaHCO_3$, pH adjusted to 7.4 with NaOH) containing antibiotics (penicillin G 100 U/ml and streptomycin 100 U/ml). Airways lacking cartilage were selected and airway smooth muscle bundles were microdissected free from surrounding tissues. Bundles were cut longitudinally and the epithelium was disrupted by gently stripping the luminal surface with a scalpel blade. Minced tissue fragments ($\sim$ 1 mm^3) were seeded into sterile 25-ml culture flasks and 2–3 ml Dulbecco's modified Eagle's medium (DMEM), containing 20% (vol/vol) FBS was added. Flasks were placed in a 6% CO_2 humidified incubator at 37°C. Culture medium was replaced every 2–3 days until cell confluence occurred (usually between 8 and 10 d). Confluent cells were passaged with 0.25% trypsin (containing 0.02% EGTA) and subcultured in DMEM with 10% FBS. Cells between passages 3 and 7 were used for all experiments.

Immunocytochemistry

ASMCs were immunolabeled for smooth muscle α-actin, smooth muscle myosin heavy chain II (Sm MHC II), or TRPV4. ASMCs were fixed with 4% formaldehyde for 10 minutes, permeabilized with methanol (−80°C), blocked with 2% BSA (in PBS), and incubated with a mouse anti–α-actin monoclonal antibody (1:100; sc-32251, lot no. B1610; Santa Cruz, Santa Cruz, CA), or a mouse anti–sm MHC II) monoclonal antibody (ab683 lot no. GR119806-2; Abcam, Cambridge, England, UK), or a rabbit anti-TRPV4 antibody (1:250; catalog no. ab39260-100, lot no. 770687; Abcam) overnight at 4°C. Cells were washed and incubated with a goat anti-mouse secondary antibody conjugated with Texas red (1:1,000; sc-27821, lot no. A2411; Santa Cruz, CA) or a goat anti-rabbit–Texas red–conjugated secondary antibody (1:1000; catalog no. ab6719, lot no. GR34115-1; Abcam) for 2 hours at room temperature in the dark. Fluorescent images were obtained using a spinning disk confocal microscope (Andor, Belfast, Northern Ireland, UK) and a 100× oil immersion objective. FITC was excited at 488 nm and Texas red at 561 nm. Immunofluorescence was not detected in cells probed with secondary antibody alone. All images were acquired at 1,024 × 1,024 pixels and were analyzed in Volocity version 6.0 (Perkin-Elmer, Waltham, MA) and ImageJ version 1.42q (NIH, Bethesda, MD).

RNA Isolation and RT-PCR

RNA was isolated and purified from primary ASMCs using an RNeasy Protect Mini Kit (Qiagen, Venlo, Limburg, Germany) according to the manufacturer's instructions. Total RNA was used to synthesize cDNA with the aid of an Omniscript reverse transcriptase kit (Qiagen) using 200 ng of RNA per reaction. PCR for TRPV1–6 and NFATc1–4 was performed using specific primer sets (QT00180782 for TRPV1, QT00187698 for TRPV2, QT01616503 for TRPV3, QT00193907 for TRPV4, QT00184590 for TRPV5, QT00185255 for TRPV6, QT02487044 for NFATc1, QT01625043 for NFATc2, QT01604148 for NFATc3, QT01805461 for NFATc4; Qiagen). Amplified PCR products were analyzed by agarose gel electrophoresis (2%) in the presence of ethidium bromide. PCR reactions always included a template-free negative control. The identity of amplified PCR fragments was confirmed by sequencing.

Confocal Calcium Imaging

ASMCs were loaded with Fluo-4 AM (4 μM) for 20 minutes at 37°C, 6% CO_2 in

the dark. Loaded cells were washed with and imaged in a physiologic Hepes-buffered solution: 146 mM NaCl, 4.7 mM KCl, 2.5 mM $CaCl_2$, 0.6 mM MgSO4, 0.15 mM NaHPO4, 0.1 mM ascorbic acid, 8 mM glucose, 10 mM Hepes (pH 7.4). Calcium imaging was performed using a multiline spinning disk confocal microscope built on an Olympus IX-70 stand equipped with a 60× oil-immersion lens and an Andor iXON charge-coupled device (CCD) camera. All experiments were performed at room temperature (22–25°C). Cells were excited at 488 nm and images were captured every 2 seconds (100-ms exposure) for a total of 200 seconds. Ca^{2+}-free experiments were performed with Ca^{2+}-free physiological Hepes-buffered solution (no added $CaCl_2$; EGTA [3 mM]). The Ca^{2+}-free solution was otherwise identical to the Hepes-buffered solution.

Cellular Proliferation Assays

Two methods were used to detect ASMC proliferation: Live cell count using trypan blue exclusion and the colorimetric 3-(4,5-dimethylthiazol-2-yl)-2,5-diphenyltetrazolium bromide (MTT) assay. For the trypan blue exclusion method, primary ASMCs were seeded into 24-well culture plates at a density of 4×10^4 cells/ml. After 24 hours, the medium was changed to new medium containing treatments or vehicle (DMSO) and cells were cultured for another 48 hours. Cells were stained with trypan blue and viable cells were counted using a hemocytometer. Four wells for each treatment group were counted. For MTT assays, ASMCs were seeded in 96-well plates at a density of 1×10^4 cells/ml in a volume of 100 μl. Six replicates per treatment were included. After 24 hours, media were replaced with fresh DMEM (100 μl) and drug treatments were added. Drug treatments were added only at the beginning of the experiment and were not repeated. Cells were allowed to proliferate for an additional 48 hours, and MTT (12 mM) was added to the wells (20 μl/well). After 4 hours of incubation at 37°C, the medium was removed and DMSO was added (150 μl/well). The plates were agitated gently at room temperature for 10 minutes. Absorbance at 590 nm (A_{590}) was read using a microplate reader (ELX800; Bio-tek, Carson City, NV).

Total Internal Reflection Fluorescence Microscopy

TRPV4 Ca^{2+} sparklets were recorded and analyzed essentially as previously described (12). Total internal reflection fluorescent microscopy (TIRFM) recordings (3-ms exposure time) were acquired using a through-the-lens total internal reflection fluorescence system built around an inverted IX-70 microscope (Olympus, Tokyo, Japan) equipped with an Olympus plan apochromatic 100× oil immersion lens (numerical aperture = 1.49) and an Andor iXON Ultra EMCCD camera. ASMCs were loaded with fluo 4-AM (4 μM) for 20 minutes at 37°C and 6% CO_2 in the dark. Cells were washed with and imaged in physiologic Hepes-buffered solution. All experiments were performed at room temperature (22–25°C). Each recording was 1,500 frames and approximately 20–40 seconds long. Recordings were processed and analyzed using a custom algorithm implemented as a plug-in (LC_Pro) for ImageJ software (14). The LC_Pro plug-in for ImageJ can be downloaded from the ImageJ Web site (http://rsbweb.nih.gov/ij/plugins/lc-pro/index.html). Ca^{2+} signal amplitude is expressed as instantaneous fluorescence (F) normalized to the baseline fluorescence (F_0), or F/F_0, of automatically detected regions of interest (ROIs). Briefly, ROIs are defined by regions with an area of 12.56 pixels^2 or greater (a circle with a radius of two pixels) appearing in at least two consecutive frames with signal rising above background. F_0 for each signal was calculated from the mean ROI intensity over the time course after subtraction of superimposed Ca^{2+} signals (14). Pseudocolor images of Ca^{2+} influx events and plots of F/F_0 versus time were created using SparkAn imaging software (a gift from Drs. Adrian Bonev and Mark T. Nelson, University of Vermont, Burlington, VT).

Proximity Ligation Assay

Colocalization of calcineurin with either TRPV4 or TRPV3 in primary ASMCs was determined using an *in situ* proximity ligation assay (PLA) detection kit (Duolink; Olink Biosciences, Inc., Uppsala, Sweden) (15). Glass slides were pretreated with a blocking solution containing 1% BSA and 1% fish gelatin in MgPSS (in mM, 140 NaCl, 5 KCl, 2 MgCl2, 10 glucose, 10 Hepes, pH 7.4 with NaOH) for 10 minutes at room temperature. Cells were allowed to adhere to glass slides for 20 minutes at 4°C and fixed with 4% formaldehyde at room temperature (10 min) followed by 120 minutes at 4°C. After washes in MgPSS, cells were permeabilized with cold methanol (−80°C) and incubated overnight in blocking solution containing paired primary antibodies: rabbit anti-TRPV4 (1:100; ab39260-100, lot no. 770,687; Abcam) or rabbit anti-TRPV3 (1:100; ab63138, lot no. 898637; Abcam) and goat anti-calcineurin/PP2B-Aβ (1:250; sc-6124, lot no. E3111; Santa Cruz) or goat anti-protein kinase C (PKC) δ (1:250; sc-213-G, lot no. G1906; Santa Cruz). After incubation in primary antibodies, cells were washed in blocking solution followed by three washes (10 min each) with 10 mM Tris, 150 mM NaCl, and 0.05% Tween 20 (pH 7.4). Cells were incubated in a humidified chamber at 37°C for 60 minutes in secondary anti-rabbit plus and anti-goat minus PLA probes and then washed three times (5 min each) with 10 mM Tris, 150 mM NaCl, and 0.05% Tween 20 (pH 7.4) at room temperature. Cells were incubated in Ligation-Ligase solution (Duolink) for 30 minutes at 37°C in a humidified chamber and then washed three times (2 min each) with 10 mM Tris, 150 mM NaCl, and 0.05% Tween 20 (pH 7.4) at room temperature. Finally, cells were incubated in amplification-polymerase solution for 100 minutes at 37°C in a humidified chamber and later washed twice for 2 minutes with 10 mM Tris and 100 mM NaCl (pH 7.5). Cells were further washed in 10 mM Tris and 100 mM NaCl (pH 7.5) for 1 minute and mounted using *in situ* mounting medium containing 4′,6-diamidino-2-phenylindole (Duolink). Fluorescent images were obtained using a spinning disk confocal microscope (Andor) and a 100× oil immersion objective. Generation of positive signal (bright red puncta) only occurred when the two PLA probes were in close proximity (< 40 nm). Excitation of fluorescent puncta was achieved with illumination at 561 nm, and autofluorescence of the cytosol was illuminated at 488 nm. Images were analyzed in Volocity imaging software version 6.0 (Perkin-Elmer). Negative control experiments were performed by omitting primary antibodies or PLA probes, and no positive signals were detected (data not shown). The density of positive puncta per cell was determined using an automated object-finding protocol in the Volocity imaging software package.

Plasmid Transfection and Live-Cell Imaging

Primary ASMCs were transfected with expression plasmids encoding NFATc3 tagged with green florescent protein (NFATc#-GFP) (Addgene no. 21,666; Addgene, Cambridge, MA) and/or the NFAT inhibitory peptide VIVIT-GFP (Addgene no. 11,106) by electroporation using a Genepulser Xcell (110 V, 25 ms pulse; Bio-Rad, Hercules, CA). Transfected cells were incubated for 48–72 hours before experimentation. Live-cell imaging was performed using a multiline spinning disk confocal microscope built on an Olympus IX-70 stand equipped with a 60× oil-immersion lens and an Andor iXON CCD camera. All experiments were performed at room temperature (22–25°C). Cells were excited at 488 nm, and images were captured every 2 seconds (250-ms exposure) for a total of 500 seconds.

Statistical Analysis

All data are expressed as the mean (± SE); "*n*" refers to the number of replicate cultures of proliferation assays or the number of cells analyzed for other experiments. Differences between the two groups of the PLA assay were determined using a Student's unpaired *t* test. Differences among multiple groups were determined using one-way or one-way repeated measures ANOVA followed by a Student-Newman-Keuls *post hoc* test. Differences were considered to be significant when *P* was less than 0.05.

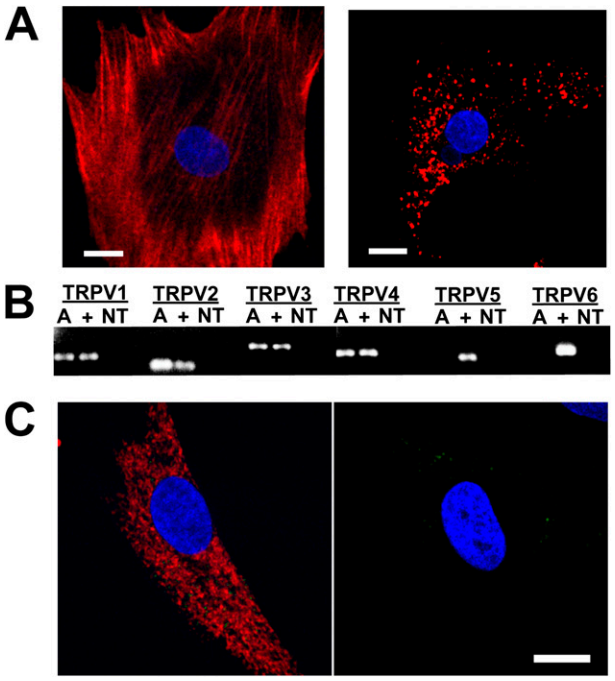

Figure 1. Vanilliod transient receptor potential channel (TRPV) 4 is present in primary airway smooth muscle cells (ASMCs). (*A*) ASMCs immunolabeled for smooth muscle α-actin (*left*) or smooth muscle myosin heavy chain II (*right*). Cell nuclei are stained with 4′,6-diamidino-2-phenylindole (DAPI; *blue*). Data are representative of at least three experiments. *Scale bar*, 10 μm. (*B*) RT-PCR demonstrating that TRPV1–4 mRNAs are present in primary ASMC cultures. TRPV5 and -6 were not detected. +, positive control cDNA (whole-brain RNA for TRPV1–4, whole-kidney RNA for TRPV5 and -6); A, ASMC cDNA; NT, no cDNA template control. Data are representative of at least three experiments. (*C*) *Left*, primary ASMCs immunolabeled for TRPV4 (*red*); *right*, little fluorescence was detected in the absence of TRPV4 primary antibody. Cell nuclei are stained with DAPI (*blue*). Data are representative of at least three experiments. *Scale bar*, 10 μm.

Results

TRPV4 Is Present and Functional in Primary ASMCs

Cells migrating out of rat airway explants after 8–10 days were spindle shaped with central oval nuclei, and displayed the typical "hill and valley" appearance of proliferative smooth muscle cells. Immunolabeling for α-actin detected parallel actin fibers and punctate expression of Sm MHC in the cytoplasm, positively identifying these cells as primary ASMCs (Figure 1A) (16). RT-PCR analysis revealed that mRNA encoding TRPV1, -2, -3, and -4 is present in these cells, whereas TRPV5 and -6 were not detected (Figure 1B). Immunolabeling for TRPV4 protein resulted in positive staining in the membrane and cytoplasm, whereas little fluorescence was present when the primary antibody was omitted (Figure 1C), demonstrating that TRPV4 channels are present in primary rat ASMCs. Due to their flat morphology and proximity of the apical and basal membranes, TRPV4-specific labeling appeared diffuse in primary ASMCs. Localization of TRPV4 in primary rat ASMCs is consistent with a prior report of functional TRPV4 channel expression in primary human ASMCs (17).

Confocal Ca^{2+} imaging was used to record the effects of the selective small-molecule TRPV4 agonist, GSK1016790A (18), on global ASMC intracellular Ca^{2+} levels. Cells were loaded with the Ca^{2+} indicator dye, Fluo-4 AM, and changes in fluorescence (F/F_0) in response to GSK1016790A (1–300 nM) were recorded. GSK1016790A caused an increase in intracellular [Ca^{2+}] (Figure 2A) that was apparent at a concentration of 10 nM and maximal at 100 nM. The relationship between [GSK1016790A] and increases in intracellular [Ca^{2+}] (F/F_0) was fitted to a sigmoidal function, which yielded a half-maximal effective concentration (EC_{50}) of 18.1 (± 2.4) nM (n = 22; Figure 2B). Additional experiments showed that the selective TRPV4 blocker, HC-067047 (500 nM) (19), essentially abolished GSK1016790A (100 nM)-induced Ca^{2+} influx, but this treatment did not diminish increases in intracellular [Ca^{2+}] in response to the Ca^{2+} ionophore ionomycin (Figures 2C and 2D). Together, these data indicate that activation of TRPV4 channels increases intracellular [Ca^{2+}] in primary ASMCs.

To determine whether the increase in intracellular [Ca^{2+}] in response to TRPV4 activity resulted from extracellular Ca^{2+} influx or release of Ca^{2+} from intracellular stores, Ca^{2+} imaging experiments were performed using

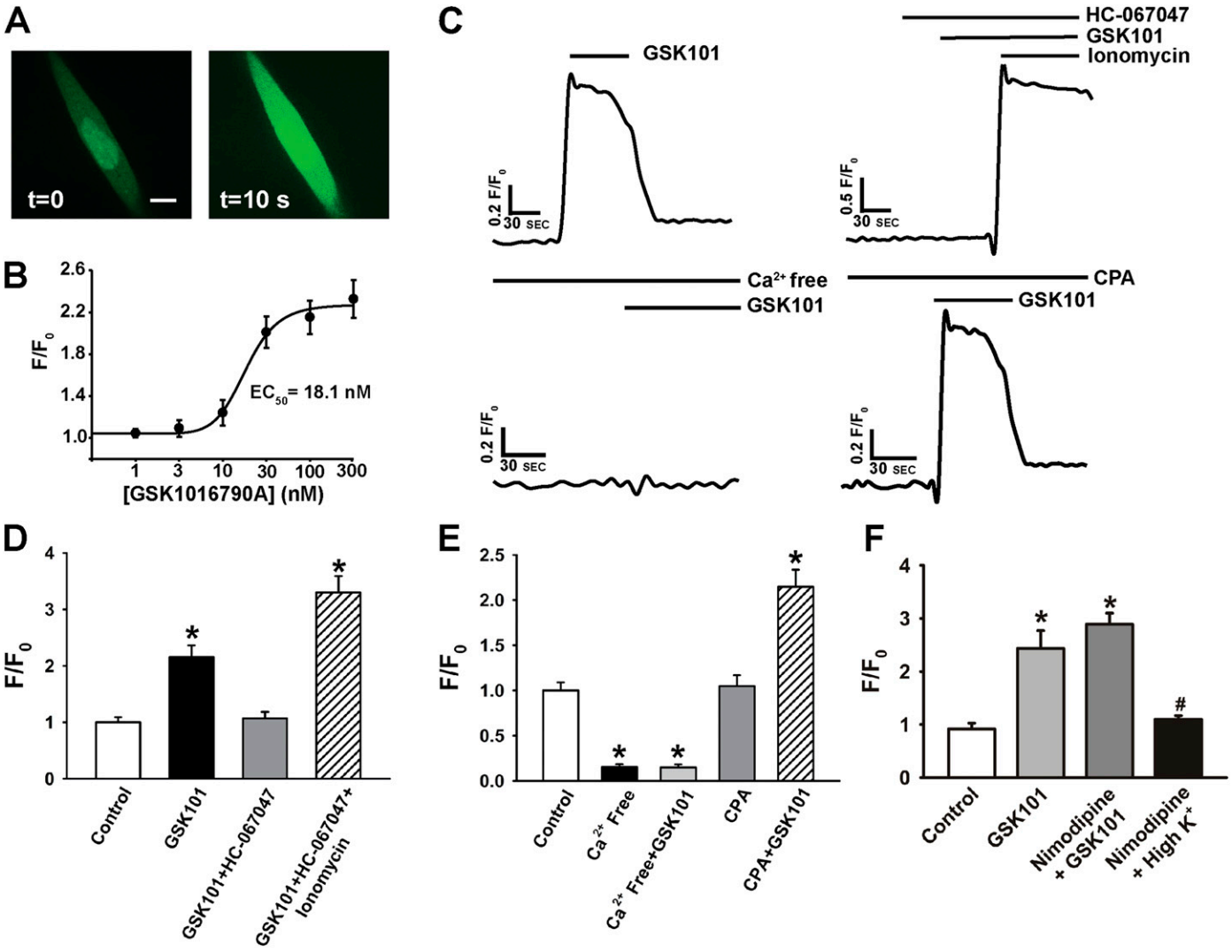

Figure 2. TRPV4 mediated Ca^{2+} influx in ASMCs. (*A*) Representative confocal images of an ASMC loaded with Ca^{2+} indicator, Fluo-4 AM, before (*left*) and 10 seconds after (*right*) administration of the TRPV4 agonist, GSK1016790A (100 nM). *Scale bar*, 10 μm. (*B*) Increase in fluorescence (F/baseline F [F_0]) stimulated by GSK1016790A is concentration dependent. Half-maximal effective concentration (EC_{50}) was 18.1 (± 2.4) nM (n = 22). (*C*) Representative recordings of F/F_0 of ASMCs loaded with Fluo 4 AM. *Top left*: administration of GSK1016790A (GSK101) (100 nM) induced an increase in intracellular Ca^{2+}. *Top right*: pretreatment with the TRPV4-selective antagonist, HC-067047 (500 nM), inhibited GSK1016790A-induced increases in intracellular Ca^{2+}, but did not prevent Ca^{2+} influx in response to administration of the Ca^{2+} ionophore ionomycin (5 μM). *Lower left*: GSK1016790A-induced Ca^{2+} increases were absent when cells were bathed in Ca^{2+}-free media. *Lower right*: depletion of intracellular Ca^{2+} stores with the sarco/endoplasmic reticulum Ca^{2+}-ATPase (SERCA) pump inhibitor, cyclopiazonic acid (CPA) (10 μM), had no effect on GSK1016790A-induced Ca^{2+} responses. (*D*) Summary of GSK1016790A (100 nM)-induced changes in F/F_0 in the presence of vehicle or HC-067047 (500 nM); $^*P < 0.05$ versus control; n = 20 cells per group. (*E*) Summary of GSK1016790A-induced changes in F/F_0 for cells bathed in Ca^{2+}-free media or treated with CPA; $^*P < 0.05$ versus control; n = 20 cells per group. (*F*) Summary data showing that GSK1016790A (100 nM)-induced increases in intracellular [Ca^{2+}] are not affected by the L-type Ca^{2+} channel blocker, nimodipine (1 μM); $^*P < 0.05$ versus control; $^{\#}P < 0.05$ versus nimodipine + GSK101; n = 3–5 cells per group. Data with *error bars* represent the mean ± SE.

Ca^{2+}-free media and the sarco/endoplasmic reticulum Ca^{2+} ATPase pump inhibitor, cyclopiazonic acid (CPA; 10 μM). GSK1016790A treatment did not increase intracellular [Ca^{2+}] when Ca^{2+} was absent from the extracellular bathing solution (Figures 2C and 2E). In contrast, pretreatment with CPA had no effect on GSK1016790A-induced increases in intracellular [Ca^{2+}] (Figures 2C and 2E). Further experiments showed that GSK1016790A-induced Ca^{2+} influx was not attenuated by the L-type Ca^{2+} channel blocker, nimodipine (1 μM) (Figure 2F). These data demonstrate that TRPV4 is a functional Ca^{2+} influx channel in primary ASMCs, and GS1016790A-mediated Ca^{2+} influx does not require the activity of L-type Ca^{2+} channels.

TRPV4 Activity Stimulates ASMC Proliferation

The effects of elevated TRPV4 activity on ASMC proliferation were determined. Cells

were treated with GSK1016790A (1–300 nM) for 48 hours in the presence of FBS (10%), and proliferation was assessed by direct live cell count (with trypan blue exclusion) and by the colorimetric MTT assay. The results of the two methods were identical and demonstrate that the TRPV4 agonist elevates proliferation of primary ASMCs in a concentration-dependent manner (Figure 3A). The EC_{50} of GSK1016790A for cellular proliferation is 27.8 (± 4.3) nM (n = 6; Figure 3A). Similar experiments were performed in the absence of FBS and demonstrate that GSK1016790A can also stimulate ASMC proliferation under these conditions with similar potency (EC_{50} = 26.4 ± 7.7 nM; n = 6; Figure 3B). Treatment with the selective TRPV4 blocker, HC-067047 (1–3,000 nM), diminished FBS (10%)-induced proliferation of ASMCs with a 50% maximal inhibitory concentration (IC_{50}) of 254.8 (± 69.6) nM (n = 6; Figure 3C). These findings suggest that basal TRPV4 activity supports proliferation of primary ASMCs under standard culture conditions.

Epoxyeicosatrienoic acids (EETs) are compounds produced from arachidonic acid by cytochrome P450 epoxygenase enzymes that are endogenous activators of TRPV4 (20). Treatment with the 11,12-EET regioisomer (500 nM; 48 h) enhanced ASMC proliferation (Figure 3D). Both 11,12-EET– and GSK1016790A-induced ASMC proliferation were abolished by blocking TRPV4 with HC-067047 (1 μM) (Figure 3D), demonstrating that an endogenously produced TRPV4 agonist can stimulate proliferation of primary ASMCs.

TRPV4 Ca^{2+} Sparklets in ASMCs

Ca^{2+} influx events through single TRPV4 channels, called TRPV4 Ca^{2+} sparklets, were recently recorded from vascular endothelial cells using confocal imaging (13) and TIRFM (12). To determine if TRPV4 Ca^{2+} sparklets are present in ASMCs, cells were loaded with fluo 4-AM and imaged using TIRFM. Imaging and analysis were performed essentially as previously described (12). Localized (mode spatial spread = 0.7 μm^2; n = 6,880 events), transient changes in fluorescence, representing Ca^{2+} microdomains at the cell surface, were recorded at low frequency (0.2 ± 0.5 Hz; n = 15) under basal conditions (Figure 4A). Event frequency was increased nearly fourfold by GSK1016790A (10 nM; 0.79 ± 0.25 Hz; n = 20; *see* Movie E1 in the online supplement). Plotting the amplitude of fluorescence change (F/F_0) of active regions as a function of time revealed that many events exhibit a plateau phase reminiscent of single channel openings recorded in patch clamp experiments (Figure 4B). Furthermore, integral amplitude levels are apparent at intervals of $\Delta F/F_0$ = 0.06, identical to levels of TRPV4 Ca^{2+} sparklets recorded from endothelial cells using TIRFM (12) (Figure 4B). The mode amplitude in the presence of GSK1016790A was $\Delta F/F_0$ = 0.18 (range, 0.06–1.98; n = 6,880 events), three times the apparent unitary amplitude ($\Delta F/F_0$ = 0.06), suggesting that the simultaneous opening of three TRPV4 channels generate the majority of the events recorded. This finding is in agreement with a recent report of cooperative TRPV4 channel gating (13).

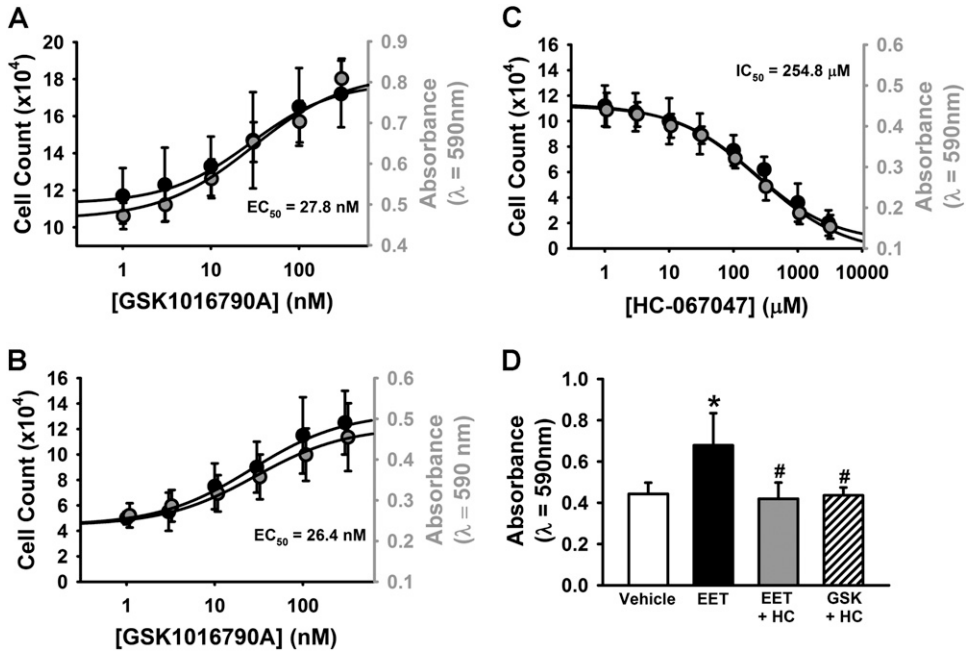

Figure 3. TRPV4 activity stimulates ASMC proliferation. (*A*) Live ASMC count (*left axis*) or 3-(4,5-dimethylthiazol-2-yl)-2,5-diphenyltetrazolium bromide (MTT) absorbance (590 nm; *right axis*) for cells treated with GSK1016790A (1–300 nM) for 48 hours in the presence of FBS (10%) (EC_{50} = 27.8 ± 4.3 nM); n = 6. (*B*) Live ASMC count and MTT absorbance for cells treated with GSK1016790A (1–300 nM) for 48 hours in the absence of FBS (EC_{50} = 26.4 ± 7.7 nM); n = 6. (*C*) Live ASMC count and MTT absorbance for cells treated with the selective TRPV4 blocker, HC-067047 (HC; 1–3,000 nM), for 48 hours in the presence of FBS (10%) (half-maximal inhibitory concentration [IC_{50}] = 254.8 ± 69.6 nM; n = 6). (*D*) MTT absorbance of ASMCs treated with the endogenous TRPV4 agonist, 11,12-epoxyeicosatrienoic acid (EET) (500 nM), or GSK 1016790A (100 nM), for 48 hours in the in the presence and absence of HC (500 nM). $^*P < 0.05$ versus vehicle; $^{\#}P < 0.05$ versus EET; n = 6 for all groups. Data with *error bars* represent the mean ± SE.

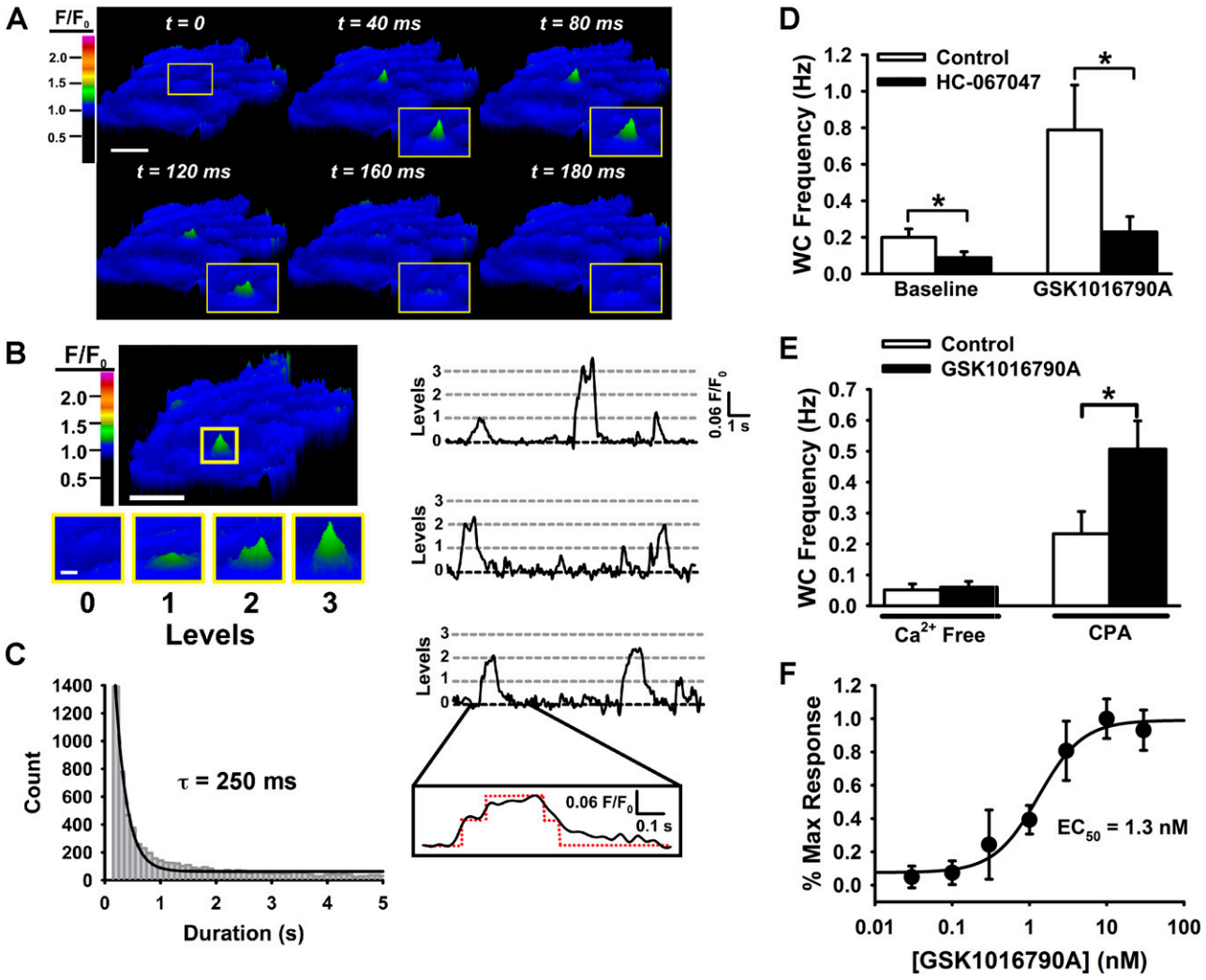

Figure 4. TRPV4 Ca^{2+} sparklets are present in ASMCs. (*A*) Representative pseudocolor time series images of a TRPV4 Ca^{2+} sparklet recorded from an ASMC using total internal reflection fluorescence microscopy (TIRFM). *Scale bar*, 10 μm. (*B*) (*Left*) Representative image showing a TRPV4 Ca^{2+} sparklet site within a region of interest (ROI) and TRPV4 Ca^{2+} sparklets with the ROI at three different amplitude (F/F_0) levels (*inset*). (*Right*) Representative plots of changes in F/F_0 for TRPV4 Ca^{2+} sparklets within an ROI as a function of time. Integral amplitude levels are indicated. *Inset* at the *bottom* shows an expanded time scale. (*C*) *Histogram* demonstrating exponential distribution of event duration (τ = 250 ms). (*D*) Summary data indicating an elevation of Ca^{2+} sparklet frequency in response to GSK1016790A. This response is diminished by HC-067047. $^*P < 0.05$. *n* = 10–20 per group. (*D*) Effect of SERCA pump inhibitor, CPA, and removal of extracellular Ca^{2+} on the basal and GSK1016790A-induced whole-cell TRPV4 Ca^{2+} sparklet frequency. $^*P < 0.05$ versus baseline; *n* = 13–20 per group. (*F*) TRPV4 Ca^{2+} sparklet frequency as a function of [GSK1016790A]. EC_{50} = 1.3 nM; *n* = 17–34. Data with *error bars* represent the mean ± SE.

Signal duration exhibited an exponential distribution, with the most frequently occurring events lasting 110 milliseconds (range, 40–5,000 ms; *n* = 6,880 events; Figure 4C). Ca^{2+} event frequency under basal conditions and in the presence of GSK1016790A was diminished by the selective TRPV4 inhibitor, HC-067047 (500 nM; *n* = 15 cells; Figure 4D). Furthermore, basal and GSK1016790A-induced Ca^{2+} events persisted after depletion of intracellular Ca^{2+} stores with CPA, but were essentially abolished when cells were bathed in Ca^{2+}-free medium, indicating that the signals were generated by Ca^{2+} influx from the extracellular solution (Figure 4E). GSK1016790A-induced increases in Ca^{2+} event frequency were concentration dependent (EC_{50} = 1.3 ± 0.2 nM; *n* = 17–34; Figure 4F). The frequency of basal and GSK1016790A-induced TRPV4 Ca^{2+} sparklets was not altered by nimpodipine (1 μM). Together, these data demonstrate that TRPV4 Ca^{2+} sparklets represent unitary Ca^{2+} influx through TRPV4 channels in ASMCs and can be recorded using TIRFM.

TRPV4 and Calcineurin Colocalize in Primary ASMCs

Experiments were performed to determine the functional significance of TRPV4 Ca^{2+} sparklets in ASMCs. A prior study demonstrated that L-type Ca^{2+} channel sparklets stimulate proliferation of arterial smooth muscle cells via the calcineurin/NFAT pathway in hypertensive animals (9). Microdomains formed by TRPV4 Ca^{2+}

sparklets could have a similar function in ASMCs if the channels are proximal to calcineurin. This hypothesis was tested using *in situ* PLA, an antibody-based technique that produces positive signals (red puncta) if targeted proteins are less than 40 nm apart (15). A substantial number of red PLA puncta were observed (42 ± 7; n = 15 cells) when ASMCs were coimmunolabeled with antibodies against calcineurin and TRPV4, indicating colocalization of these two proteins (Figures 5A and 5B). In contrast, few puncta were observed when ASMCs were coimmunolabeled with calcineurin and TRPV3 antibodies (2 ± 1, n = 15 cells), or with antibodies binding to PKCδ and TRPV4 (7 ± 2, n = 30 cells), indicating that these proteins do not colocalize in primary ASMCs (Figures 5A and 5B). These data indicate that TRPV4 channels specifically colocalize with calcineurin in primary ASMCs, supporting the hypothesis that TRPV4 Ca^{2+} sparklets can activate calcineurin activity in these cells.

Nuclear Translocation of NFATc3 after TRPV4 Activation Stimulates ASMC Proliferation

Members of the NFAT family of transcription factors are important for arterial smooth muscle cell differentiation and proliferation (6, 7), but it is not known if these proteins have a similar function in ASMCs. Using RT-PCR analysis, we find that mRNAs encoding the four Ca^{2+}/calcineurin–dependent NFAT isoforms (NFATc1–4) are present in primary ASMCs (Figure 6A). NFATc activation is accomplished by the Ca^{2+}-dependent phosphatase calcineurin, which dephosphorylates cytosolic NFAT to allow nuclear translocation. To determine if TRPV4 channels are involved in the calcineurin/NFAT pathway, primary ASMCs were transfected with an expression plasmid encoding an NFATc3-GFP fusion protein. In unstimulated cells, NFATc3-GFP was confined to the cytosol (Figure 6B). However, after treatment with GSK1016790A (100 nM), nearly all of the NFATc3-GFP protein rapidly translocated to the nucleus (Figures 6B–6D). Nuclear translocation in response to GSK1016790A is blocked when cells are pretreated with the selective TRPV4 antagonist, HC-067047 (500 nM) (Figures 6B and 6D), and does not occur when Ca^{2+} is not present in the bathing solution (Figure 6D), indicating that TRPV4-mediated Ca^{2+} influx stimulates nuclear translocation of NFATc3 in ASMCs. VIVIT is an inhibitory peptide that prevents interaction between NFAT and calcineurin (21). Cotransfecting cells with NFATc3-GFP and a plasmid expressing VIVIT-GFP prevented nuclear translocation of NFATc3-GFP in response to TRPV4 activation (Figures 6B and 6D), providing further evidence that TRPV4-mediated Ca^{2+} influx causes nuclear translocation of NFATc3-GFP by stimulating calcineurin activity.

The effects of TRPV4-mediated NFATc nuclear translocation on primary ASMC proliferation were investigated using the MTT assay. Proliferation of ASMCs was increased by FBS (10%; 48 h), and was further stimulated by GSK1016790A (100 nM) (Figure 6E). The calcineurin-inhibitory compound, cyclosporine A (CsA; 10 μM), blocked GSK1016790A-induced ASMC proliferation (Figure 6E). Furthermore, expression of VIVIT-GFP had no effect on FBS (10%)-induced ASMC proliferation, but blocked GSK1016790A-induced increases in cell number (Figure 6E). Together, these data indicate that Ca^{2+} influx via TRPV4 stimulates ASMC proliferation by activating calcineurin-dependent nuclear translocation of NFAT.

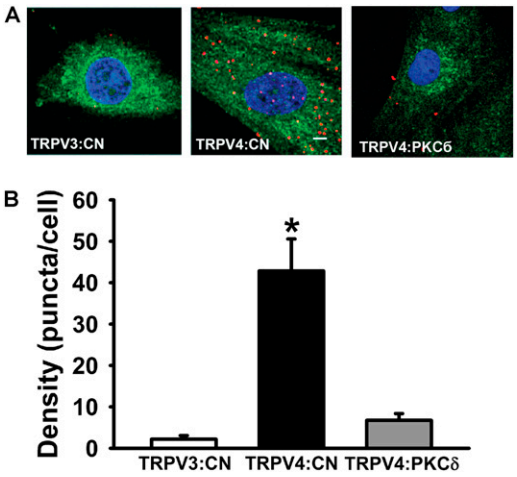

Figure 5. TRPV4 colocalizes with the Ca^{2+}/calmodulin–activated phosphatase calcineurin in ASMCs. (*A*) Example images of *in situ* proximity ligation assay (PLA) performed by coimmunolabeling ASMCs with antibodies against TRPV3 and calcineurin (CN) (*left*), TRPV4 and CN (*middle*), or TRPV4 and protein kinase C (PKC) δ (*right*). The presence of abundant PLA puncta (*red spots*) demonstrates that TRPV4 and CN are no more than 40 nm apart in ASMCs. Nuclei are stained with DAPI (*blue*) and cellular autofluorescence is *green*. *Scale bar*, 10 μm. (*B*) Summary of PLA puncta counts for both groups. *$P < 0.05$ versus TRPV3:CN; n = 15–30 cells per group. Data with *error bars* represent the mean ± SE.

Discussion

Severe asthma is associated with ASMC proliferation, ultimately leading to remodeling and irreversible obstruction of airways. This disease process is poorly understood, and no specific treatments are currently available. Findings reported here reveal a novel signaling pathway involving TRPV4 channels, the Ca^{2+}/calmodulin–dependent phosphatase calcineurin, and the NFAT family of transcription factors that stimulates proliferation of ASMCs. Our data show that TRPV4 channels are present and functional in primary ASMCs, and are capable of generating TRPV4 Ca^{2+} sparklets. More interestingly, we find that TRPV4 channels colocalize with calcineurin in ASMCs, and that TRPV4-mediated NFAT nuclear translocation is associated with primary ASMC proliferation. These results indicate that TRPV4-dependent Ca^{2+} signals generated proximal to calcineurin activate NFAT transcriptional pathways to stimulate ASMC proliferation. Significantly, our findings provide a mechanistic framework involving TRPV4 channels and the

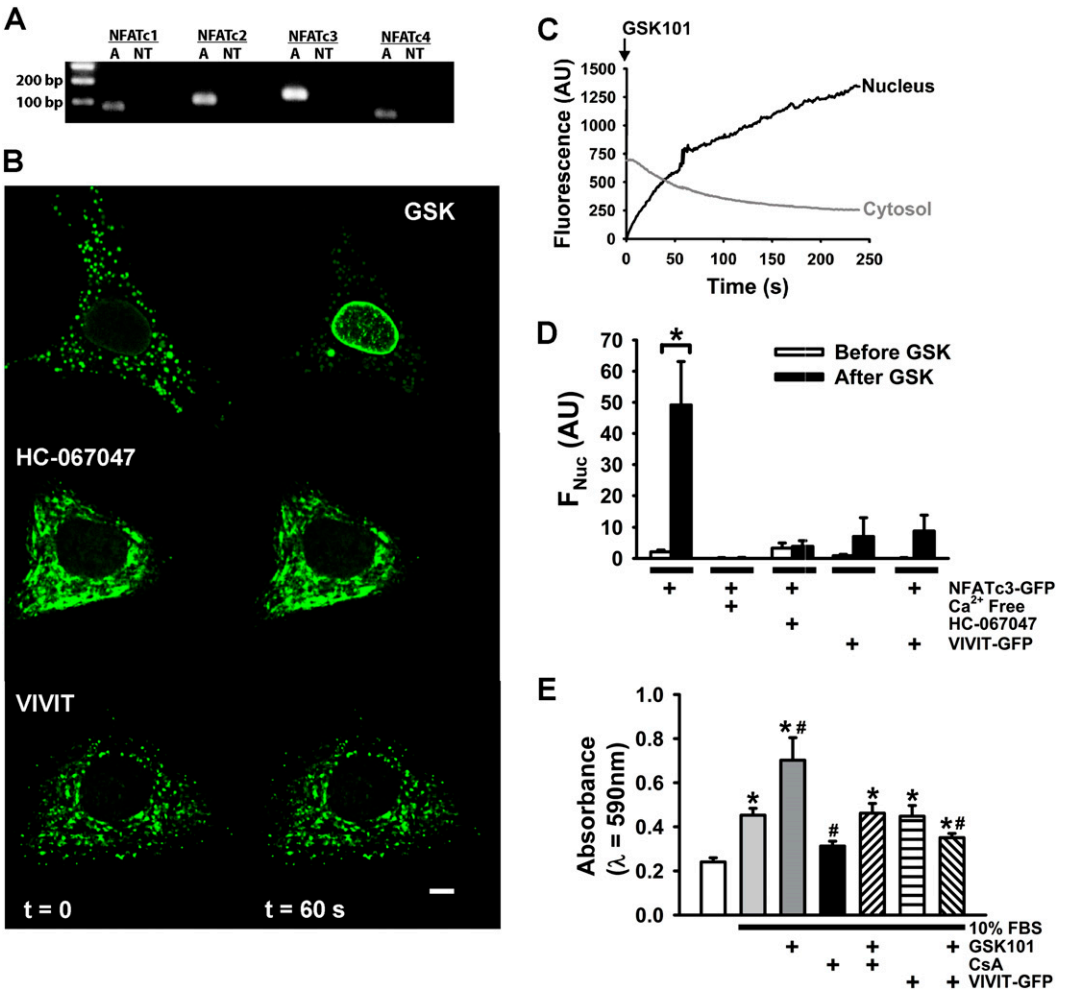

Figure 6. Nuclear factor of activated T cells (NFAT) nuclear translocation after TRPV4 activation stimulates ASMC proliferation (*A*) RT-PCR demonstrating that NFATc1–4 are present in mRNA isolated from primary ASMCs. A, ASMC cDNA; NT, no cDNA template control. Data are representative of at least three experiments. (*B*) Example images demonstrating the effects of TRPV4 activity on the localization of NFATc3 tagged with green florescent protein (NFATc3-GFP) in ASMCs. *Top*: representative images of an ASMC transfected with NFATc3-GFP before (*left*) and after (*right*) treatment with GSK1016790A (GSK) (100 nM). *Middle*: same experiment performed in the presence of HC-067047. *Bottom*: same experiment performed in cells coexpressing NFATc3-GFP and the VIVIT peptide. *Scale bar*, 10 μm. (*C*) Representative time course of changes in cytosolic and nuclear fluorescence (AU, arbitrary units) for an ASMC expressing NFATc3-GFP after administration of GSK1016790A (GSK101) (100 nM). (*D*) Summary of GSK1016790A (GSK; 100 nM)-induced changes in nuclear fluorescence (AU) for ASMCs expressing NFATc3-GFP under normal conditions, in Ca^{2+}-free solution, in the presence of HC-067047 (500 nM), and in cells coexpressing NFATc3-GFP and VIVIT-GFP. *$P < 0.05$ versus before GSK; n = 3–10 in each group. (*E*) MTT absorbance of ASMCs cultured for 48 hours without FBS, or in the presence of FBS (10%) and treated with GSK1016790A (100 nM), the calcineurin inhibitor, cyclosporine A (CsA; 10 μM), or cotransfected with a VIVIT-GFP expression plasmid. *$P < 0.05$ versus 0% FBS; #$P < 0.05$ versus untreated 10% FBS; n = 6. Data with *error bars* represent the mean ± SE.

calcineurin/NFAT pathway for therapeutic development to prevent or resolve asthma-induced airway remodeling.

ASMC hypertrophy and hyperplasia have long been recognized as primary factors leading to irreversible narrowing of airways during severe asthma (4, 22). The current findings are the first to demonstrate that Ca^{2+} influx via TRPV4 stimulates ASMC proliferation, suggesting that elevated channel activity associated with the disease could contribute to airway remodeling. TRPV4 is activated by synthetic chemical compounds (GSK1016790A [18] and 4α-phorbol 12,13-didecanoate [23]), endogenously generated substances (i.e., EETs [20] and Bisandrographolide, a compound extracted from the *Andrographis paniculata* plant used in traditional Asian medicine [24]), warm temperatures (25), and hypotonic conditions (26, 27). We report here that GSK1016790A and 11,12-EET enhance FBS-induced ASMC proliferation by activating TRPV4. More interestingly, we find that TRPV4 activity can also stimulate ASMC proliferation in the absence of FBS, indicating that TRPV4-mediated cation influx alone is sufficient to stimulate cellular proliferation. In addition, we also show that inhibition of TRPV4 attenuates FBS-induced ASMC proliferation, suggesting that TRPV4 activity stimulated by substances present in FBS or by warm temperatures (37°C) support the growth of ASMCs. Increased TRPV4 activity could result from elevated levels of EETs produced by the airway epithelium or other inflammatory cells during asthma.

Alternatively, fluids covering airway surfaces in patients with asthma are hypotonic compared with healthy control subjects (28), suggesting that changes in osmolality could trigger TRPV4-mediated ASMC proliferation associated with the disease. Consistent with this possibility, TRPV4 channels present in primary human ASMCs are thought to mediate Ca^{2+} influx in response to hypotonic solution (17). Although additional experiments are needed to link TRPV4 activity with ASMC proliferation *in vivo*, our initial findings support the concept that blocking of TRPV4 could be useful for preventing asthma-induced airway remodeling.

TRPV4 channels are highly permeable to Ca^{2+} ions (relative permeability to Ca^{2+} vs. Na^{+} [PCa:PNa] $\approx$ 6:1 [26]), and likely influence cellular Ca^{2+} homeostasis when present and active. Ca^{2+} signals can be global (i.e., continuous throughout the cytosol) and persistent, or can be spatially restricted to specific regions for brief periods of time. Localized, transient Ca^{2+} signals have significant functional impact in smooth muscle cells. For example, Ca^{2+} sparks, generated by Ca^{2+} ions released from ryanodine receptors located on the sarcoplasmic reticulum of arterial smooth muscle cells, activate large-conductance Ca^{2+}-activated K^{+} channels to hyperpolarize the sarcolemma and dilate cerebral arteries (29). Another example of local Ca^{2+} signaling is provided by an elegant series of studies from the Santana laboratory, demonstrating that L-type Ca^{2+} channel sparklets (unitary Ca^{2+} influx events that occur through $Ca_V1.2$ channels [10]) in arterial smooth muscle cells regulate basal global Ca^{2+} levels (11, 30, 31) and proliferation of arterial myocytes during hypertension (9; for review *see* Ref. 32). This body of work also shows that persistently active L-type Ca^{2+} channel sparklet sites are intricate signaling complexes organized by A-kinase anchor proteins (AKAPs), such as AKAP150 scaffolding proteins (33). Ca^{2+} influx through single TRPV4 channels can be recorded from endothelial cells using high-speed confocal (13) or TIRF microscopy (12) as distinctive signals called TRPV4 Ca^{2+} sparklets. A recent study demonstrates that TRPV4 Ca^{2+} sparklets in mesenteric arteries mediate endothelium-dependent vasodilation (13).

Ca^{2+} sparks and Ca^{2+} sparklets are distinct Ca^{2+} signaling events. Ca^{2+} sparks require Ca^{2+} release from intracellular stores through ryanodine receptors and are much larger in amplitude compared with L-type Ca^{2+} channel and TRPV4 Ca^{2+} sparklets, whereas Ca^{2+} sparklets are generated by Ca^{2+} influx from the extracellular space. L-type Ca^{2+} channel sparklets are much smaller in amplitude and spatial spread compared with TRPV4 Ca^{2+} sparklets, and the two signals are easily distinguished (for review *see* Ref. 34). A study demonstrating that TRPV4-mediated Ca^{2+} influx increases the frequency of Ca^{2+} sparks in cerebral artery smooth muscle cells to cause vasodilation (35) suggests the intriguing possibility that TRPV4 Ca^{2+} sparklets could influence Ca^{2+} spark activity by Ca^{2+}-induced Ca^{2+} release.

Findings reported here are the first recordings of TRPV4 Ca^{2+} sparklets in smooth muscle cells. We find that the unitary amplitude and duration of TRPV4 Ca^{2+} sparklets in smooth muscle cells imaged with TIRFM are similar to those recorded from primary human endothelial cells using the same technique (12). Furthermore, in agreement with recordings obtained from the intact endothelium (13), our findings provide evidence for cooperative gating of TRPV4 channels in ASMCs. We also find that higher concentrations of GSK1016790A were required to stimulate changes in global Ca^{2+} level (EC_{50} = 18.1 nM) versus those required to increase TRPV4 Ca^{2+} sparklet frequency (EC_{50} = 1.3 nM). This is expected, as global Ca^{2+} increases are a result of the summation of individual Ca^{2+} influx events. More interestingly, we find that TRPV4 channels colocalize with Ca^{2+}/calmodulin–dependent phosphatase calcineurin in ASMCs. Intriguingly, this close association ($<$ 40 nm) of a Ca^{2+} influx pathway and a Ca^{2+}-dependent signaling molecule suggests that Ca^{2+} microdomains created by TRPV4 Ca^{2+} sparklets could activate calcineurin in ASMCs with significant functional impact.

The primary function of Ca^{2+}/calmodulin–activated calcineurin is dephosphorylation of NFAT proteins (36), a family of transcription factors involved in immune cell activation (37) and proliferation of vascular smooth muscle cells (6, 38). The possible consequences of TRPV4 Ca^{2+} sparklet–mediated activation of calcineurin were investigated by recording the effects of TRPV4 activity on NFAT activation and ASMC proliferation. In quiescent cells, Ca^{2+}/calcineurin–dependent NFAT isoforms (NFATc1–4) are highly phosphorylated and reside in the cytosol, but, in response to specific Ca^{2+} signals, activated calcineurin docks with and dephosphorylates NFAT, allowing nuclear translocation and initiation of proliferative transcriptional programs (39). Distinctive Ca^{2+} signals regulate the calcineurin/NFAT pathway in different types of cells. For example, in nonexcitable cells, store-operated Ca^{2+} influx pathways are critically important for NFAT activity (40), whereas, in native smooth muscle cells, blocking of $Ca_V1.2$ channels inhibits NFAT nuclear accumulation, indicating an obligate role for voltage-dependent Ca^{2+} influx (41, 42). Our findings show that mRNAs encoding all four Ca^{2+}/calcineurin–dependent NFAT isoforms are present in primary ASMCs. We also show that TRPV4 stimulation causes nuclear translocation of NFATc3-GFP in ASMCs by a process that requires extracellular Ca^{2+} influx and association of calcineurin with NFAT. Furthermore, we report that inhibition of calcineurin activity or preventing association of calcineurin with NFAT blocks ASMC proliferation in response to TRPV4 activation. These findings indicate that Ca^{2+} influx through TRPV4 activates calcineurin, which dephosphorylates NFAT to initiate nuclear translocation and stimulate ASMC proliferation. Higher concentrations of GSK1016790A were needed to induce proliferation compared with TRPV4 Ca^{2+} sparklet activation, perhaps because GSK1016790A binds to proteins present in the tissue culture medium, diminishing bioavailability during the cellular proliferation. Alternatively, GSK1016790A may not be completely stable at 37°C for 48 hours, diminishing effectiveness of the compound in cellular assays. Furthermore, the data indicating the effects of CsA on ASMC proliferation should be interpreted with caution, as the MTT assay used for this experiment measures cellular metabolism rather than cell number. Although data shown in Figure 3 indicate excellent correspondence between the MTT assay and direct live cell count using trypan blue exclusion, it is possible that effects of CsA on mitochondrial function could be confounding. Regardless, close association of TRPV4 Ca^{2+} sparklet sites and calcineurin reported here suggests that TRPV4 Ca^{2+} sparklets are the fundamental Ca^{2+} signals responsible for initiating the

calcineurin/NFAT proliferative pathway in ASMCs, a previously unrecognized mechanism of NFAT activation.

In summary, our findings show that Ca^{2+} influx via TRPV4 stimulates proliferation of ASMCs by activating the calcineurin/NFAT-signaling pathway, identifying TRPV4 and calcineurin/NFAT as potential targets for the prevention of asthma-induced airway remodeling. Selective inhibitors of calcineurin, such as CsA and FK506, effectively block the NFAT pathway, but the immunosuppressive effects of these drugs are incompatible with long-term use for patients with asthma. In contrast, a recent study, showing that selective blocking of TRPV4 in rodents prevents and resolves heart failure–induced pulmonary edema without serious side effects, provides support for the therapeutic potential of TRPV4 pharmacology (43). Although additional work is necessary, the current findings provide a clear mechanistic context for future *in vivo* studies to directly test this hypothesis. ■

Author disclosures are available with the text of this article at www.atsjournals.org.

Acknowledgments: The authors thank Ms. Jennifer J. Robinson for technical assistance, Drs. Mark S. Taylor and Michael Francis for supplying LC_Pro image analysis software, Dr. Mark T. Nelson and Adrian Bonev for SparkAn software, and Dr. Kevin S. Thorneloe for valuable comments on the manuscript.

References

1. Moreno RH, Hogg JC, Pare PD. Mechanics of airway narrowing. *Am Rev Respir Dis* 1986;133:1171–1180.
2. Loren ML, Leung PK, Cooley RL, Chai H, Bell TD, Buck VM. Irreversibility of obstructive changes in severe asthma in childhood. *Chest* 1978;74:126–129.
3. Warner SM, Knight DA. Airway modeling and remodeling in the pathogenesis of asthma. *Curr Opin Allergy Clin Immunol* 2008;8:44–48.
4. Huber HL, Koessler KK. The pathology of bronchial asthma. *Arch Intern Med* 1922;30:689–760.
5. Owens GK, Kumar MS, Wamhoff BR. Molecular regulation of vascular smooth muscle cell differentiation in development and disease. *Physiol Rev* 2004;84:767–801.
6. Yellaturu CR, Ghosh SK, Rao RK, Jennings LK, Hassid A, Rao GN. A potential role for nuclear factor of activated T-cells in receptor tyrosine kinase and G-protein–coupled receptor agonist–induced cell proliferation. *Biochem J* 2002;368:183–190.
7. Liu Z, Zhang C, Dronadula N, Li Q, Rao GN. Blockade of nuclear factor of activated T cells activation signaling suppresses balloon injury–induced neointima formation in a rat carotid artery model. *J Biol Chem* 2005;280:14700–14708.
8. Rao A, Luo C, Hogan PG. Transcription factors of the NFAT family: regulation and function. *Annu Rev Immunol* 1997;15:707–747.
9. Nieves-Cintron M, Amberg GC, Navedo MF, Molkentin JD, Santana LF. The control of Ca^{2+} influx and NFATc3 signaling in arterial smooth muscle during hypertension. *Proc Natl Acad Sci USA* 2008;105:15623–15628.
10. Navedo MF, Amberg GC, Westenbroek RE, Sinnegger-Brauns MJ, Catterall WA, Striessnig J, Santana LF. Ca(v)1.3 channels produce persistent calcium sparklets, but Ca(v)1.2 channels are responsible for sparklets in mouse arterial smooth muscle. *Am J Physiol Heart Circ Physiol* 2007;293:H1359–H1370.
11. Navedo MF, Amberg GC, Votaw VS, Santana LF. Constitutively active L-type Ca^{2+} channels. *Proc Natl Acad Sci USA* 2005;102: 11112–11117.
12. Sullivan MN, Francis M, Pitts NL, Taylor MS, Earley S. Optical recording reveals novel properties of GSK1016790a-induced vanilloid transient receptor potential channel TRPV4 activity in primary human endothelial cells. *Mol Pharmacol* 2012;82:464–472.
13. Sonkusare SK, Bonev AD, Ledoux J, Liedtke W, Kotlikoff MI, Heppner TJ, Hill-Eubanks DC, Nelson MT. Elementary Ca^{2+} signals through endothelial TRPV4 channels regulate vascular function. *Science* 2012;336:597–601.
14. Francis M, Qian X, Charbel C, Ledoux J, Parker JC, Taylor MS. Automated region of interest analysis of dynamic $Ca(2)^{+}$ signals in image sequences. *Am J Physiol Cell Physiol* 2012;303:C236–C243.
15. Fredriksson S, Gullberg M, Jarvius J, Olsson C, Pietras K, Gustafsdottir SM, Ostman A, Landegren U. Protein detection using proximity-dependent DNA ligation assays. *Nat Biotechnol* 2002;20:473–477.
16. Halayko AJ, Salari H, Ma X, Stephens NL. Markers of airway smooth muscle cell phenotype. *Am J Physiol* 1996;270:L1040–L1051.
17. Jia Y, Wang X, Varty L, Rizzo CA, Yang R, Correll CC, Phelps PT, Egan RW, Hey JA. Functional TRPV4 channels are expressed in human airway smooth muscle cells. *Am J Physiol Lung Cell Mol Physiol* 2004;287:L272–L278.
18. Thorneloe KS, Sulpizio AC, Lin Z, Figueroa DJ, Clouse AK, McCafferty GP, Chendrimada TP, Lashinger ES, Gordon E, Evans L, *et al*. N-((1s)-1-{[4-((2s)-2-{[(2,4-dichlorophenyl)sulfonyl]amino}-3-hydroxypropanoyl)-1-piperazinyl]carbonyl}-3-methylbutyl)-1-benzothiophene-2-carboxamide (GSK1016790A), a novel and potent transient receptor potential vanilloid 4 channel agonist induces urinary bladder contraction and hyperactivity: part I. *J Pharmacol Exp Ther* 2008;326:432–442.
19. Everaerts W, Zhen X, Ghosh D, Vriens J, Gevaert T, Gilbert JP, Hayward NJ, McNamara CR, Xue F, Moran MM, *et al*. Inhibition of the cation channel TRPV4 improves bladder function in mice and rats with cyclophosphamide-induced cystitis. *Proc Natl Acad Sci USA* 2010; 107:19084–19089.
20. Watanabe H, Vriens J, Prenen J, Droogmans G, Voets T, Nilius B. Anandamide and arachidonic acid use epoxyeicosatrienoic acids to activate TRPV4 channels. *Nature* 2003;424:434–438.
21. Aramburu J, Yaffe MB, Lopez-Rodriguez C, Cantley LC, Hogan PG, Rao A. Affinity-driven peptide selection of an NFAT inhibitor more selective than cyclosporin a. *Science* 1999;285:2129–2133.
22. Benayoun L, Druilhe A, Dombret MC, Aubier M, Pretolani M. Airway structural alterations selectively associated with severe asthma. *Am J Respir Crit Care Med* 2003;167:1360–1368.
23. Watanabe H, Davis JB, Smart D, Jerman JC, Smith GD, Hayes P, Vriens J, Cairns W, Wissenbach U, Prenen J, *et al*. Activation of TRPV4 channels (hVRL-2/mTRP12) by phorbol derivatives. *J Biol Chem* 2002;277:13569–13577.
24. Smith PL, Maloney KN, Pothen RG, Clardy J, Clapham DE. Bisandrographolide from *Andrographis paniculata* activates TRPV4 channels. *J Biol Chem* 2006;281:29897–29904.
25. Watanabe H, Vriens J, Suh SH, Benham CD, Droogmans G, Nilius B. Heat-evoked activation of TRPV4 channels in a HEK293 cell expression system and in native mouse aorta endothelial cells. *J Biol Chem* 2002;277:47044–47051.
26. Strotmann R, Harteneck C, Nunnenmacher K, Schultz G, Plant TD. OTRPC4, a nonselective cation channel that confers sensitivity to extracellular osmolarity. *Nat Cell Biol* 2000;2:695–702.
27. Liedtke W, Choe Y, Marti-Renom MA, Bell AM, Denis CS, Sali A, Hudspeth AJ, Friedman JM, Heller S. Vanilloid receptor–related osmotically activated channel (VR-OAC), a candidate vertebrate osmoreceptor. *Cell* 2000;103:525–535.
28. Joris L, Dab I, Quinton PM. Elemental composition of human airway surface fluid in healthy and diseased airways. *Am Rev Respir Dis* 1993;148:1633–1637.
29. Nelson MT, Cheng H, Rubart M, Santana LF, Bonev AD, Knot HJ, Lederer WJ. Relaxation of arterial smooth muscle by calcium sparks. *Science* 1995;270:633–637.
30. Amberg GC, Navedo MF, Nieves-Cintron M, Molkentin JD, Santana LF. Calcium sparklets regulate local and global calcium in murine arterial smooth muscle. *J Physiol* 2007;579:187–201.
31. Navedo MF, Amberg GC, Nieves M, Molkentin JD, Santana LF. Mechanisms underlying heterogeneous Ca^{2+} sparklet activity in arterial smooth muscle. *J Gen Physiol* 2006;127:611–622.
32. Santana LF, Navedo MF, Amberg GC, Nieves-Cintron M, Votaw VS, Ufret-Vincenty CA. Calcium sparklets in arterial smooth muscle. *Clin Exp Pharmacol Physiol* 2008;35:1121–1126.

33. Navedo MF, Nieves-Cintron M, Amberg GC, Yuan C, Votaw VS, Lederer WJ, McKnight GS, Santana LF. AKAP150 is required for stuttering persistent Ca^{2+} sparklets and angiotensin ii–induced hypertension. *Circ Res* 2008;102:e1–e11.
34. Sullivan MN, Earley S. TRP channel Ca^{2+} sparklets: fundamental signals underlying endothelium-dependent hyperpolarization. *Am J Physiol Cell Physiol* 2013;305:C999–C1008.
35. Earley S, Heppner TJ, Nelson MT, Brayden JE. TRPV4 forms a novel Ca^{2+} signaling complex with ryanodine receptors and BKCA channels. *Circ Res* 2005;97:1270–1279.
36. Graef IA, Chen F, Chen L, Kuo A, Crabtree GR. Signals transduced by Ca(2+)/calcineurin and NFATc3/c4 pattern the developing vasculature. *Cell* 2001;105:863–875.
37. Shaw JP, Utz PJ, Durand DB, Toole JJ, Emmel EA, Crabtree GR. Identification of a putative regulator of early T cell activation genes. *Science* 1988;241:202–205.
38. Nilsson LM, Sun ZW, Nilsson J, Nordstrom I, Chen YW, Molkentin JD, Wide-Swensson D, Hellstrand P, Lydrup ML, Gomez MF. Novel blocker of NFAT activation inhibits IL-6 production in human myometrial arteries and reduces vascular smooth muscle cell proliferation. *Am J Physiol Cell Physiol* 2007;292:C1167–C1178.
39. Zhu J, McKeon F. Nucleocytoplasmic shuttling and the control of NF-AT signaling. *Cell Mol Life Sci* 2000;57:411–420.
40. Serafini AT, Lewis RS, Clipstone NA, Bram RJ, Fanger C, Fiering S, Herzenberg LA, Crabtree GR. Isolation of mutant T lymphocytes with defects in capacitative calcium entry. *Immunity* 1995;3: 239–250.
41. Gomez MF, Stevenson AS, Bonev AD, Hill-Eubanks DC, Nelson MT. Opposing actions of inositol 1,4,5-trisphosphate and ryanodine receptors on nuclear factor of activated T-cells regulation in smooth muscle. *J Biol Chem* 2002;277:37756–37764.
42. Stevenson AS, Gomez MF, Hill-Eubanks DC, Nelson MT. NFAT4 movement in native smooth muscle: a role for differential Ca(2+) signaling. *J Biol Chem* 2001;276:15018–15024.
43. Thorneloe KS, Cheung M, Bao W, Alsaid H, Lenhard S, Jian MY, Costell M, Maniscalco-Hauk K, Krawiec JA, Olzinski A, *et al*. An orally active TRPV4 channel blocker prevents and resolves pulmonary edema induced by heart failure. *Sci Transl Med* 2012;4:159ra148.